

SMM313 Numerical Methods: Applications

Coursework Report

Group 4

Gael Chan, Huiqi Li, Nathaniel Stephenson, Wincy So

March 2025

Contents

Contents	2
List of Tables	2
List of Figures	2
1 Exercise 1	3
1.1 Task 1	3
1.2 Task 2	3
1.3 Task 3	5
1.4 Task 4	5
1.5 Task 5	9
2 Exercise 2	12
References	15

List of Tables

1 Expected Lower Bound Price and Delta	5
2 Expected Geometric Asian Call Option Price and Delta	5
3 Comparison of Direct Simulation and Control Variate Methods	7
4 Correlation coefficient between arithmetic option prices, lower bounds, and geometric option prices	8
5 Comparison of Simulated and Exact Prices	8
6 Arithmetic Asian option price with (a) lower bound and (b) geometric Asian option price as control variates	8
7 Arithmetic Asian option sensitivity with sensitivity of (a) lower bound and (b) geometric Asian option price as control variates	8
8 Comparison of Discrete LB vs. Continuous LB (Trapezoid)	11
9 Results for Barrier $U = 160$	13
10 Results for Barrier $U = 170$	13
11 Continuously Monitored Up-and-Out Barrier Call Option Prices	14

List of Figures

1 Convergence of the Discrete LB to the Continuous LB.	11
2 Scatter plot of Monte Carlo payoffs versus antithetic variate payoffs for the up-and-out barrier call option	12
3 Convergence of Discretely Monitored UOC Prices	14

1 Exercise 1

1.1 Task 1

The expression for the likelihood ratio (LR) first-order sensitivity estimator with respect to S_0 of: (a) the arithmetic Asian option with discounted payoff

$$\mu'_{c,S_0} = \mathbb{E}_{S_0} \left(f(A_n) \frac{d \ln g_{S_0}(S_n)}{dS_0} \right)$$

$$\mu'_{c,S_0} = \mathbb{E}_{S_0} \left(e^{-rT} \left(\frac{1}{n} \sum_{k=1}^n S_k - K \right)^+ \frac{\zeta(S_1 | S_0)}{S_0 \sigma \sqrt{t_1}} \right)$$

(b) The lower bound

$$\mu'_{c,S_0} = \mathbb{E}_{S_0} \left(f(LB_n) \frac{d \ln g_{S_0}(S_n)}{dS_0} \right)$$

$$\mu'_{c,S_0} = \mathbb{E}_{S_0} \left(e^{-rT} \left(\frac{1}{n} \sum_{k=1}^n S_k - K \right) \mathbf{1}_{\{(\prod_{k=1}^n S_k)^{1/n} > K\}} \frac{\zeta(S_1 | S_0)}{S_0 \sigma \sqrt{t_1}} \right)$$

(c) The geometric Asian option with discounted payoff

$$\mu'_{c,S_0} = \mathbb{E}_{S_0} \left(f(G_n) \frac{d \ln g_{S_0}(S_n)}{dS_0} \right)$$

$$\mu'_{c,S_0} = \mathbb{E}_{S_0} \left(e^{-rT} \left(\left(\prod_{k=1}^n S_k \right)^{1/n} - K \right)^+ \frac{\zeta(S_1 | S_0)}{S_0 \sigma \sqrt{t_1}} \right)$$

The **pathwise method** relies on the relationship between the payoff and the parameter of interest θ , which is the initial stock price S_0 . The payoff function for the lower bound is given as

$$LB_n = e^{-rT} \left(\frac{1}{n} \sum_{k=1}^n S_k - K \right) \Big|_{G > K} \quad \text{where } G \text{ is the geometric average price of the underlying}$$

asset. This means the payoff of the option is zero unless the geometric average price of the underlying asset is also greater than the strike price K . This indicator function introduces discontinuity at $G = K$. The pathwise method requires the payoff function to be continuous and differentiable with respect to S_0 . Therefore, it cannot be applied to obtain an unbiased estimator for the first-order sensitivity of LB_n with respect to S_0 .

1.2 Task 2

Finding first sensitivities enable the application of risk management in hedging strategies, utilizing the Greeks. Specifically, when differentiating with respect to S_0 , this finds the delta of the option and will indicate how reactive the option price is to the change in the initial stock price.

Deriving the formula for the first sensitivities with respect to S_0 of the lower bound (a) and the geometric Asian option (b):

(a) Lower Bound Option Sensitivity

$$\frac{d}{dS_0} \mathbb{E}(LB_n) = \frac{d}{dS_0} \left(\frac{S_0 e^{-rT}}{n} \sum_{k=1}^n e^{\mu_k + \frac{\sigma_k^2}{2}} N(b + a_k) \right) - \frac{d}{dS_0} (K e^{-rT} N(b))$$

Due to the product rule and the fact that b is a function of S_0 , the term $\frac{db}{dS_0}$ appears. This yields:

$$\begin{aligned} \frac{d}{dS_0} \mathbb{E}(LB_n) &= \frac{e^{-rT}}{n} \sum_{k=1}^n e^{\mu_k + \frac{\sigma_k^2}{2}} N(b + a_k) \\ &\quad + \frac{S_0 e^{-rT}}{n} \sum_{k=1}^n e^{\mu_k + \frac{\sigma_k^2}{2}} N'(b + a_k) \frac{db}{dS_0} \\ &\quad - K e^{-rT} N'(b) \frac{db}{dS_0} \end{aligned}$$

Where b is given by:

$$b = \frac{\ln(S_0/K) + (r - \frac{\sigma^2}{2})\bar{T}}{\bar{\sigma}\sqrt{\bar{T}}} \quad \Rightarrow \quad \frac{db}{dS_0} = \frac{1}{S_0 \bar{\sigma} \sqrt{\bar{T}}}$$

Additionally, the standard normal CDF is:

$$N(x) = \int_{-\infty}^x \frac{1}{\sqrt{2\pi}} e^{-t^2/2} dt \quad \Rightarrow \quad \frac{d}{dS_0} N(x) = n(x) = \frac{1}{\sqrt{2\pi}} e^{-x^2/2}$$

Therefore,

$$\begin{aligned} \frac{d}{dS_0} \mathbb{E}(LB_n) &= \frac{e^{-rT}}{n} \sum_{k=1}^n e^{\mu_k + \frac{\sigma_k^2}{2}} N(b + a_k) \\ &\quad + \frac{S_0 e^{-rT}}{n} \sum_{k=1}^n e^{\mu_k + \frac{\sigma_k^2}{2}} \frac{1}{\sqrt{2\pi}} e^{-\frac{(b+a_k)^2}{2}} \cdot \frac{1}{S_0 \bar{\sigma} \sqrt{\bar{T}}} \\ &\quad - K e^{-rT} \cdot \frac{1}{\sqrt{2\pi}} e^{-b^2/2} \cdot \frac{1}{S_0 \bar{\sigma} \sqrt{\bar{T}}} \end{aligned}$$

Factoring and simplifying:

$$\begin{aligned} \frac{d}{dS_0} \mathbb{E}(LB_n) &= e^{-rT} \left[\frac{1}{n} \sum_{k=1}^n e^{\mu_k + \frac{\sigma_k^2}{2}} N(b + a_k) \right. \\ &\quad \left. + \frac{1}{n} \sum_{k=1}^n e^{\mu_k + \frac{\sigma_k^2}{2}} \cdot \frac{1}{\bar{\sigma} \sqrt{\bar{T}} 2\pi} e^{-\frac{(b+a_k)^2}{2}} - K \cdot \frac{1}{S_0 \bar{\sigma} \sqrt{\bar{T}} 2\pi} e^{-b^2/2} \right] \end{aligned}$$

(b) Geometric Asian Option Sensitivity

$$\frac{d}{dS_0} \mathbb{E}(G_n) = \frac{d}{dS_0} \left[S_0 e^{(r - \frac{\sigma^2}{2} + \frac{\bar{\sigma}^2}{2})\bar{T} - rT} N(d) \right] - \frac{d}{dS_0} \left[K e^{-rT} N(d - \bar{\sigma} \sqrt{\bar{T}}) \right]$$

Where

$$d = \frac{\ln(S_0/K) + (r - \frac{\sigma^2}{2} + \bar{\sigma}^2)\bar{T}}{\bar{\sigma} \sqrt{\bar{T}}} \quad \Rightarrow \quad \frac{dd}{dS_0} = \frac{1}{S_0 \bar{\sigma} \sqrt{\bar{T}}}$$

Then, by product and chain rule:

$$\begin{aligned} \frac{d}{dS_0} \mathbb{E}(G_n) &= e^{(r - \frac{\sigma^2}{2} + \frac{\bar{\sigma}^2}{2})\bar{T} - rT} N(d) \\ &\quad + S_0 e^{(r - \frac{\sigma^2}{2} + \frac{\bar{\sigma}^2}{2})\bar{T} - rT} \cdot \frac{1}{\sqrt{2\pi}} e^{-d^2/2} \cdot \frac{1}{S_0 \bar{\sigma} \sqrt{\bar{T}}} \\ &\quad - K e^{-rT} \cdot \frac{1}{\sqrt{2\pi}} e^{-(d - \bar{\sigma} \sqrt{\bar{T}})^2/2} \cdot \frac{1}{S_0 \bar{\sigma} \sqrt{\bar{T}}} \end{aligned}$$

And simplifying:

$$\frac{d}{dS_0} \mathbb{E}(G_n) = e^{-rT} \left[e^{(r - \frac{\sigma^2}{2} + \frac{\bar{\sigma}^2}{2})\bar{T}} \left(N(d) + \frac{1}{\bar{\sigma}\sqrt{\bar{T}2\pi}} e^{-d^2/2} \right) - K \cdot \frac{1}{S_0 \bar{\sigma} \sqrt{\bar{T}2\pi}} e^{-(d - \bar{\sigma}\sqrt{\bar{T}})^2/2} \right]$$

Using the lower bound is an estimate that lies above the geometric Asian option because of its geometric mean property but less than that of an arithmetic Asian option. However, the arithmetic variation requires Monte Carlo simulation and hence more computational power. When prices in a portfolio have larger correlations, the geometric and arithmetic options are more closely estimated. (Curran (1994))

1.3 Task 3

These first sensitivities (deltas) and their original forms are used in simulation with the parameters $S_0 = 100$, $r = 0.04$, $\sigma = 0.3$, $K = [90, 100, 110]$, $T = 1$, $n = [4, 12, 50]$ in MATLAB to produce the following results:

n	Price			Delta		
	$K = 90$	$K = 100$	$K = 110$	$K = 90$	$K = 100$	$K = 110$
4	15.032	9.2449	5.291	0.76687	0.57648	0.39682
12	14.136	8.2345	4.3702	0.76575	0.56715	0.36875
50	13.798	7.8490	4.0268	0.77045	0.56335	0.35684

Table 1: Expected Lower Bound Price and Delta

n	Price			Delta		
	$K = 90$	$K = 100$	$K = 110$	$K = 90$	$K = 100$	$K = 110$
4	14.525	8.8315	4.971	0.74248	0.56288	0.38356
12	13.602	7.8021	4.0382	0.75131	0.55277	0.35439
50	13.263	7.4155	3.6945	0.75580	0.54899	0.34226

Table 2: Expected Geometric Asian Call Option Price and Delta

As discussed in Task 2, the lower bound estimates are greater than that of the geometric estimates in the table. But the geometric estimate will never be greater than the lower bound. Additionally, the lower bound will never be greater than the arithmetic.

All these methods have a trade-off of speed for accuracy. Part of this is clear when looking in Task 2 at the equations for the expected lower bound price, the expected geometric option price and their deltas. The lower bound contains a summation that will take a longer time to execute than a more standard geometric option, especially as the number of monitoring points increases.

1.4 Task 4

In Question 4, the control variate method is employed to enhance the computational efficiency of the Monte Carlo Simulation for the pricing and first sensitivity analysis of Arithmetic Asian Options. It leverages the sampling uncertainty of a known estimate to reduce the sampling

uncertainty of a related, but unknown, quantity of interest.

Methodology

- Monte Carlo simulation: A large number of independent simulated paths are generated to approximate the arithmetic Asian option payoff.
- Construction of control variable: Identify an additional variable (control variate) with a known expected value that is strongly correlated with the original payoff. Computing the estimator with

$$C_b^{(j)} = C^{(j)} - b(P^{(j)} - \mu_P). \quad (1)$$

Achieve the optimal b^* through regression

- Control Variates Used: Lower Bound Control Variate (Approach a): Leveraging the near-perfect linear correlation (approximately 0.9999) with the arithmetic Asian option payoff. Geometric Asian Option Control Variate (Approach b): Employs the geometric Asian option payoff, exhibiting a correlation of approximately 0.9932 with the arithmetic Asian option payoff.

Results and Discussion

Standard Error and Accuracy

For the bond price, using the lower bound as a control variate (approach a) consistently yields standard errors around 10^{-4} , significantly lower than those obtained with the geometric Asian option (approach b), which are typically around 10^{-3} . Consequently, arithmetic Asian estimates with approach (a) generally achieve accuracy to at least two decimal places for 95% confidence intervals, except the case ($K=90$, $n=12$). In contrast, approach (b) achieves at least one decimal place accuracy consistently, except for the case ($K=90$, $n=50$). For the first sensitivity, there is similar results that using a lower bound help achieve the standard errors around 10^{-5} , however, only 10^{-4} with approach b.

Impact of Monitoring Frequency and Strike Price

For the price, estimates become more precise with increased monitoring frequency (n), as the standard errors decrease consistently across both approaches. Increasing the strike price (K) leads to lower call option prices, reflecting the inverse relationship between strike prices and in-the-money likelihood. The sensitivity of call prices to underlying asset changes also diminishes with higher strike prices, as options become progressively out-of-the-money. The option has little intrinsic value and a lower chance to finish in-the-money when the strike price is getting higher. thus a lower delta. However, as we could see in the table, the standard error of delta estimation increases with increase of the number of observations. This might subject to the calculations involved in the likelihood ratio method and in adjusting payoffs with the control variate. It might introduce numerical instabilities, particularly when dealing with the intricacies of path-dependent options like Asians calls, the control variate might fail to capture the path dependencies effectively.

Correlation and Variance Reduction

For an estimator combining payoff and control variate, the minimal variance achievable is $\text{Var}(X - \alpha(Y - E[Y])) = \text{Var}(X)(1 - \rho_{XY}^2)$ where ρ_{XY} is the correlation between the payoff and control variate. Hence, a higher correlation yields greater variance reduction, directly aligning with observed empirical results [Xu \(2023\)](#).

From the table, it is evident that the correlation between arithmetic Asian option and lower bound is higher than that of arithmetic Asian option and geometric Asian option. The correlation between the lower bound and arithmetic Asian option prices is exceptionally high at 0.99999 (at $k=90$, $n=4$), suggesting an almost linear relationship, enabling near-maximal

variance reduction. Similar experiments [Akos Horvath \(2016\)](#) confirm that such a nearly perfect correlation significantly diminishes estimation errors, practically eliminating variance and greatly enhancing estimator efficiency.

The correlation between arithmetic and geometric Asian option prices is 0.99934 (at $k=90$, $n=4$), also very high, leading to substantial efficiency gains with residual estimator variance approximately 0.132% of the original variance (calculated as $1 - \rho^2$).

Efficiency Gain

The efficiency ratio evaluates comparative efficiency between two computational approaches by considering their squared standard errors and computational times. (As we can see from the last column of table 6 and table 7) In both price and delta estimation process, the efficiency ratios are all smaller than 1. For $k=90$ and $n=4$, the efficiency ratio is 0.018813 for price estimation and 0.023635 for first sensitivity estimation. It implies that approach a is more efficient compared to approach. As we could see from the table, direct simulation takes substantially longer (3.6437s for Price, 4.1246s for Sensitivity) using 10^7 simulations. Control Variate (a) drastically reduces computational time (0.13564s for Price, 0.14545s for Sensitivity) using only 10^5 simulations, including an additional 10^4 simulations (Mb) for estimating the optimal control variate coefficient. Control Variate (b) offers even faster price calculation (0.081312s) but slightly slower sensitivity calculation (0.08819s). The standard error of Control Variate (a) for both price and sensitivity are substantially lower than that of direct simulation, approximately 27 times reduction in price estimation error and 40 times reduction in sensitivity estimation error (as we can see in table 3). Control Variate (b) significantly improves accuracy compared to direct simulation, although it is notably less accurate than method (a), reducing the standard error by around 2.6 times for price and approximately 3.9 times for sensitivity compared to direct simulation. Both control variate methods provide immense efficiency gains relative to direct simulation.

Comparison between Arithmetic Asian option price and Exact Lower Bound Price

As tabe 5 shows, the arithmetic Asian option prices simulated through Monte Carlo closely align with the theoretical LB prices. Regardless of varying strike prices (K) and frequency of observation (n), the absolute discrepancies are small (0.003–0.005). Maximum difference observed: approximately 0.054% and the minimum difference observed: approximately 0.029%. Such marginal differences suggest the LB provides a robust, highly reliable approximation to the arithmetic Asian option price. Also, a higher number of monitoring points (n) slightly reduces both the simulated and LB prices yet maintains their close relationship. This demonstrates the stability and accuracy of LB across various discretizations frequencies. The exact lower bound method serves as a highly reliable benchmark or proxy for the arithmetic Asian option price, considered a suitable control variate for estimating Arithmetic Asian option price.

	Direct Simulation		Control Variate			
	Price	Sensitivity	Price (a)	Price (b)	Sensitivity (a)	Sensitivity (b)
$K = 90, n = 4$	15.03	0.75529201	15.037	15.036	0.755916	0.7558002
Time consumption	3.6437s	4.124606s	0.13566s	0.81312s	0.14545s	0.08819s
Standard Error	0.0054369	0.00061477	0.00002311	0.0020544	1.52368×10^{-5}	1.53826×10^{-4}
Number of simulations	$M = 1E7$	$M = 1E7$	$M = 1E5$ $Mb = 1E4$	$M = 1E5$ $Mb = 1E4$	$M = 1E5$ $Mb = 1E4$	$M = 1E5$ $Mb = 1E4$

Table 3: Comparison of Direct Simulation and Control Variate Methods

Arithmetic - Lower Bound			
	4	12	50
90	0.99999	0.99999	0.99999
100	0.99999	0.99999	0.99999
110	0.99998	0.99998	0.99997
Arithmetic - Geometric			
	4	12	50
90	0.99932	0.99937	0.99935
100	0.99912	0.99918	0.99918
110	0.99872	0.99875	0.99862

Table 4: Correlation coefficient between arithmetic option prices, lower bounds, and geometric option prices

K	n	Simulated Price (a)	Exact Price Lower Bound	Absolute Difference	Relative Difference
90	4	15.037	15.032	0.005	0.033%
90	12	14.14	14.136	0.004	0.028%
90	50	13.802	13.798	0.004	0.029%
100	4	9.2499	9.2449	0.005	0.054%
100	12	8.2385	8.2345	0.004	0.049%
100	50	7.8524	7.849	0.0034	0.043%

Table 5: Comparison of Simulated and Exact Prices

K	n	Price		Standard Error		95% Confidence Interval				Efficiency Ratio
		(a)	(b)	(a)	(b)	Lower		Upper		
90	4	15.037	15.039	0.00019164	0.002053	15.036	15.037	15.035	15.043	0.18813
90	12	14.14	14.142	0.00018687	0.0018074	14.14	14.14	14.138	14.145	0.022326
90	50	13.802	13.803	0.00017579	0.0017367	13.802	13.803	13.8	13.807	0.015016
100	4	9.2499	9.2509	0.00021985	0.0019362	9.2492	9.2503	9.2471	9.2547	0.026129
100	12	8.2385	8.2384	0.00016991	0.0016429	8.2381	8.2388	8.2352	8.2417	0.01788
100	50	7.8524	7.8519	0.00015899	0.0015811	7.8521	7.8527	7.8488	7.855	0.013067
110	4	5.2959	5.2969	0.00023586	0.0018321	5.2954	5.2964	5.2933	5.3005	0.030641
110	12	4.375	4.3746	0.00021818	0.0015417	4.3746	4.3754	4.3716	4.3777	0.033074
110	50	4.0318	4.0332	0.00021674	0.0014662	4.0314	4.0323	4.0304	4.0361	0.028151

Table 6: Arithmetic Asian option price with (a) lower bound and (b) geometric Asian option price as control variates

K	n	Delta		Standard Error		95% Confidence Interval				Efficiency Ratio
		(a)	(b)	(a)	(b)	Lower		Upper		
90	4	0.755909	0.756251	1.45047e-05	1.58797e-04	0.75588	0.75594	0.75579	0.75641	0.023635
90	12	0.765903	0.765635	2.58765e-05	2.23255e-04	0.76585	0.76595	0.76553	0.76643	0.015856
90	50	0.770583	0.770631	4.47423e-05	4.08072e-04	0.77050	0.77067	0.77014	0.77183	0.012803
100	4	0.576503	0.576488	1.93540e-05	1.47040e-04	0.57647	0.57654	0.57615	0.57672	0.032061
100	12	0.567174	0.567160	2.44321e-05	2.13996e-04	0.56712	0.56722	0.56671	0.56755	0.015055
100	50	0.563315	0.563036	3.96810e-05	3.85483e-04	0.56324	0.56339	0.56207	0.56359	0.013499
110	4	0.396768	0.396758	2.11959e-05	1.30081e-04	0.39673	0.39681	0.39659	0.39712	0.029395
110	12	0.368607	0.368564	2.82256e-05	1.96205e-04	0.36855	0.36966	0.36844	0.36920	0.033166
110	50	0.356593	0.356470	5.00318e-05	3.62639e-04	0.35650	0.35669	0.35654	0.35795	0.025299

Table 7: Arithmetic Asian option sensitivity with sensitivity of (a) lower bound and (b) geometric Asian option price as control variates

1.5 Task 5

In Exercise 1 Q5, we worked on the lower bound on the value of an arithmetic Asian option under continuous versus discrete monitoring.

- **Discrete Lower Bound**, $E(\text{LB}_n)$, follows from *Curran's formula*. It assumes the underlying asset S is observed at n equally spaced time points over $[0, T]$.
 - **Continuous Lower Bound**, $E(\text{LB}_\infty)$, follows from *Thompson's formula*. It holds in the limit as $n \rightarrow \infty$ when the option is monitored continuously. Mathematically, it is defined via a one-dimensional integral that can be evaluated numerically (by integral or a trapezoidal rule).
1. We Implement $E(\text{LB}_\infty)$ in MATLAB through numerical integration (using both the built-in `integral(...)` function and a trapezoidal rule).
 2. Compute $E(\text{LB}_n)$ for increasing $n = 2^2, 2^3, 2^4, \dots$

Recall from Thompson's formula (equation (7) in the CW question) that the continuous lower bound $E(\text{LB}_\infty)$ for the arithmetic Asian option, we numerically evaluate the integral

$$\int_0^T \exp(-r(T-t)) N\left(\frac{-\gamma + \sigma t - \frac{\sigma t^2}{2T}}{\sqrt{T/3}}\right) dt$$

we used the built-in `integral` function in MATLAB for numerical integration over the interval $[0, T]$ and T is set as 1 here, it converges to

$$E(\text{LB}_\infty) \approx 7.7270,$$

We next verified Thompson's continuous lower bound formula numerically by using a *trapezoidal rule* to approximate the integral. Specifically, we:

- Partition the interval $[0, T]$ into n equally spaced subintervals of width $\Delta t = T/n$.
- Evaluate the integrand at each grid point

$$t_0 = 0, \quad t_1 = \Delta t, \quad t_2 = 2 \Delta t, \quad \dots, \quad t_n = n \Delta t = T.$$

- Multiply each integrand value by a *trapezoidal weight*. Specifically, the end points carry a half weight, while intermediate points carry a full weight:

$$w_0 = w_n = \frac{1}{2} \Delta t, \quad w_i = \Delta t, \quad (1 \leq i \leq n-1).$$

- Sum these weighted integrand evaluations to approximate the integral,

$$\int_0^T f(t) dt \approx \sum_{i=0}^n w_i f(t_i).$$

- Finally, combine the integral result with Thompson's second term $-K e^{-rT} N(\dots)$ to obtain the continuous lower bound $E(\text{LB}_\infty)$.

We performed these steps in MATLAB for a range of n values ($2^2, 2^3, \dots, 2^{20}$). As n grows, the trapezoidal-rule estimate converges to the same numerical value we obtain using MATLAB's built-in `integral(...)` function (i.e., approximately 7.727).

We computed the discrete lower bound $E(\text{LB}_n)$ from Curran's formula (equation (3) in the coursework), we define a function `lowerbound` in MATLAB and iterate over `n` values for $2^2, 2^3, \dots, 2^{20}$ and then compare with the continuous bound $E(\text{LB}_\infty)$.

Figure 1 and Table 8 illustrate how the discrete lower bound $E(\text{LB}_n)$ converges to the continuous lower bound $E(\text{LB}_\infty)$, as we increase n from 2^2 up to 2^{20} . We observe several notable aspects:

Convergence Analysis of Discrete vs. Continuous Lower Bounds

Figure 1 and Table 8 illustrate how the *discrete* lower bound $E(\text{LB}_n)$ converges to the *continuous* lower bound $E(\text{LB}_\infty)$ (about 7.727) as n increases from 2^2 up to 2^{20} .

- **Large Overshoot at Small n .**

When $n = 2^2$, the discrete LB is about 9.24, whereas the continuous LB is 7.626. When there is very few monitoring dates, the discrete LB tends to overestimate the payoff relative to continuous monitoring. In volatile markets ($\sigma = 0.3$), sparse sampling increases the likelihood of capturing extreme values (spikes, drops) in the underlying asset price S . This inflates the arithmetic average, leading to a higher LB estimate. While continuous LB integrates over the entire time interval $[0, T]$ could effectively averaging out extreme fluctuations, which reduces volatility-induced overestimation. Recall the Adjusted Time \bar{T} and Volatility $\bar{\sigma}$ in Curran's discrete LB formula.

$$\bar{T} = \frac{(n+1)\delta}{2} \quad \text{and} \quad \bar{\sigma} = \sigma \sqrt{\frac{2n+1}{3n}},$$

where $\delta = \frac{T}{n}$ when n is small, $\bar{\sigma}$ is large, which inflates the volatility adjustment and increases $N(b + a_k)$ in the summation, raising the discrete LB.

- **Monotonic Convergence from Above.**

As n doubles, $E(\text{LB}_n)$ steadily decreases toward 7.727, reducing the error by around half or more each time. At $n = 2^5$, the difference is only 0.19; at $n = 2^{10}$, around 0.006. Indicates that in denser monitoring when $n \rightarrow \infty$, it smooths out fluctuations, converging to the continuous case. The absolute difference

$$\Delta_n = |E(\text{LB}_n) - E(\text{LB}_\infty)|.$$

decreases by approximately half each time indicates an $O(1/n)$ convergence rate, where the error scales inversely with n and leads to a linear convergence.

- **Convergence Differences Between Discrete and Continuous LB Methods.**

The convergence behavior of the discrete LB and continuous LB (trapezoidal rule) towards the MATLAB built-in integral result (≈ 7.727) differs due to their underlying mathematical structures and rates of convergence. As mentioned above, the discrete LB relies on an arithmetic average over n monitoring points. Its error often decreases on the order of $1/n$ because each time n doubles, the overshoot typically shrinks by about half. However, with sparse monitoring (when n is small) and higher volatility, the discrete LB is more prone to capturing outlier price spikes and thus overshooting the continuous LB. By contrast, the continuous LB estimated via the trapezoidal rule can converge on the order of $1/n^2$ as the integrand is relatively smooth. Hence, the trapezoidal method benefits from the integral's smoothness, having rapid error reduction as the partition is refined.

$n = 2^k$	Discrete LB	Continuous LB(Trap)	Difference	Time(Discrete)	Time(Continuous)
2^2	9.2449	7.6258	1.6192	0.0016295	0.0002229
2^3	8.4877	7.7017	0.78601	0.0023636	0.0004559
2^4	8.1078	7.7206	0.38719	0.0007561	0.0003832
2^5	7.9175	7.7254	0.19215	0.0007378	0.0003762
2^6	7.8223	7.7266	0.09572	0.0023864	0.0034200
2^7	7.7746	7.7269	0.04770	0.0011435	0.0000638
2^8	7.7508	7.7269	0.02390	0.0016629	0.0000771
2^9	7.7389	7.7270	0.01190	0.0025636	0.0000403
2^{10}	7.7329	7.7270	0.00590	0.0008403	0.0000585
2^{11}	7.7299	7.7270	0.00300	0.0190130	0.0001211
2^{12}	7.7285	7.7270	0.00150	0.0230550	0.0002366
2^{13}	7.7277	7.7270	0.00080	0.0424430	0.0003256
2^{14}	7.7273	7.7270	0.00040	0.0715700	0.0015162
2^{15}	7.7271	7.7270	0.00020	0.1262500	0.0018094
2^{16}	7.7271	7.7270	0.00010	0.2505400	0.0016831
2^{17}	7.7270	7.7270	4.6562e-05	0.4827500	0.0041126
2^{18}	7.7270	7.7270	2.3281e-05	1.1256000	0.0070996
2^{19}	7.7270	7.7270	1.1641e-05	2.2039000	0.0161946
2^{20}	7.7270	7.7270	5.8203e-06	3.9129000	0.0277230

Table 8: Comparison of Discrete LB vs. Continuous LB (Trapezoid)

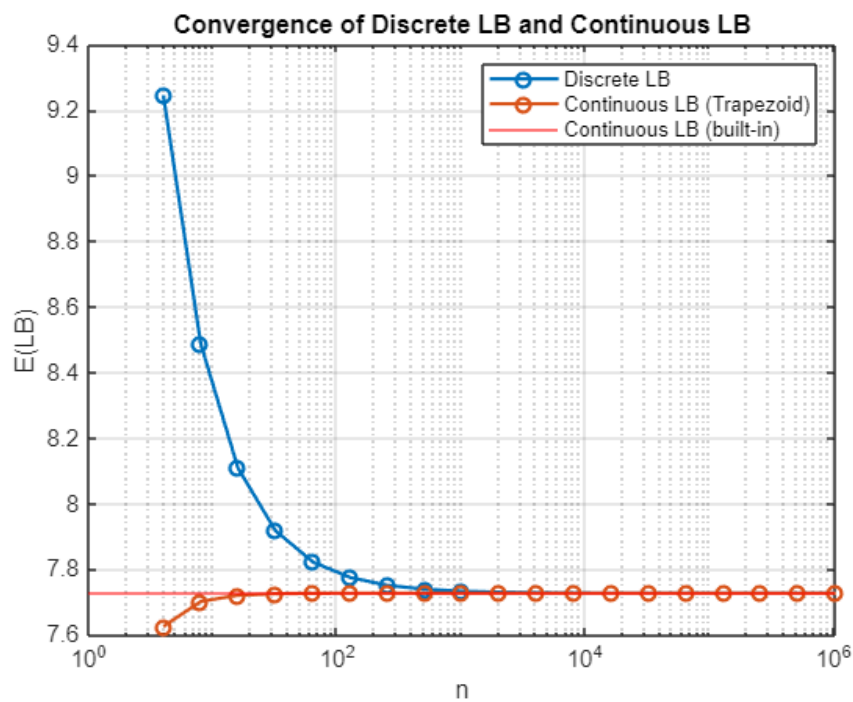


Figure 1: Convergence of the Discrete LB to the Continuous LB.

2 Exercise 2

In this exercise, we have implemented the **antithetic variate technique** to enhance the efficiency and accuracy of the Monte Carlo Simulation. This variance reduction method generates paired simulation by using standard normal variates $Z^{(j)}$ and their antithetic counterparts $-Z^{(j)}$. By introducing negative correlation between the simulated paths, the technique reduces the variance of the estimated payoffs. The discounted payoffs from each pair of paths are averaged to produce a more stable and efficient estimate of the option price:

$$\hat{\mu}_{CAV}(M) = \frac{1}{M} \sum_{j=1}^M \frac{C^{(j)} + \tilde{C}^{(j)}}{2}$$

This method reduces variance by balancing high and low estimates from correlated paths. (Glasserman (2004)) To examine the relationship between the option prices estimated by the crude MC simulation and their corresponding antithetic variate (AV) outputs, we computed the correlation coefficient between them by using the MATLAB code as below:

```
r_3 = corrcoef(U0,U0AntVar)
```

The resulting correlation matrix confirmed a strong negative correlation, with $r_3 = -0.8622$. This negative dependence between the paired simulations is an essential factor in the effectiveness of the antithetic variates technique, as it ensures that the fluctuations in one path tend to be offset by the other, thereby reducing the overall variance of the option price estimator.

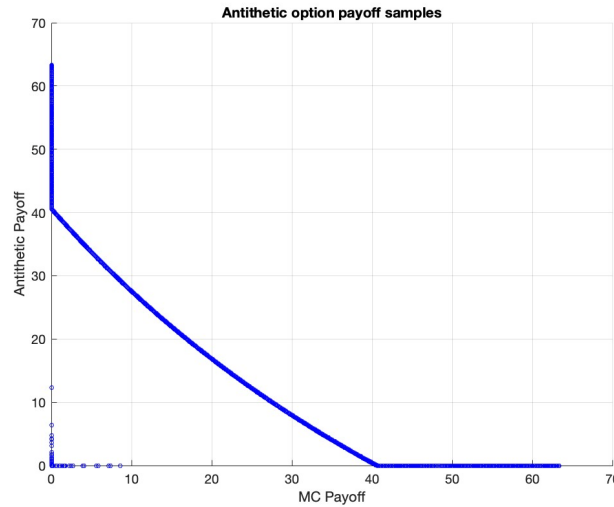


Figure 2: Scatter plot of Monte Carlo payoffs versus antithetic variate payoffs for the up-and-out barrier call option

We also generated a scatter plot of their payoffs (see Figure 2) to better study the relationship between the payoffs of the original and antithetic paths for the up-and-out barrier call option. The plot reveals a strong inverse relationship, which is characteristic of the antithetic variates technique. However, the presence of the barrier introduces a distinct pattern in the payoff distribution. The points clustered at the origin represent scenarios where both paths knock out, resulting in zero payoffs for both. There is a large cluster of points along the axes, where one payoff is zero due to the path knocking out, while the corresponding antithetic path results in a positive payoff. This behaviour reflects the discontinuous nature of barrier options, where crossing the barrier level results in the option becoming worthless. The remaining payoffs exhibit a non-linear inverse relationship, contrasting with the smoother and more linear behaviour

typically observed in options without discontinuities, such as Asian options. These features indicate that while antithetic variates remain effective in reducing variance for barrier options, their impact is moderated by the discrete knock-out condition, which introduces discontinuities in the payoff correlation. This observation is consistent with the computed correlation coefficient of $r_3 = -0.8622$, as discussed previously.

Table 9 and Table 10 show the comparison of Crude Monte Carlo (MC) and Antithetic Variates Monte Carlo simulation results for the up-and-out barrier call option with barrier level $U = 160$ and 170 respectively. Price estimates, standard errors, and 95% confidence intervals are reported for increasing number of equally spaced monitoring intervals n throughout the timespan of the option.

n	Crude Monte Carlo (MC)			Antithetic Variate Monte Carlo (AVMC)		
	Price	Std Error	95% CI	Price	Std Error	95% CI
4	18.636	0.013552	(18.609, 18.662)	18.617	0.0044380	(18.609, 18.626)
8	18.522	0.013506	(18.495, 18.548)	18.516	0.0045775	(18.507, 18.525)
16	18.401	0.013457	(18.375, 18.428)	18.410	0.0047176	(18.401, 18.419)
32	18.313	0.013408	(18.286, 18.339)	18.315	0.0048318	(18.306, 18.325)
64	18.215	0.013360	(18.189, 18.241)	18.223	0.0049378	(18.213, 18.233)
128	18.170	0.013322	(18.144, 18.196)	18.151	0.0050206	(18.141, 18.161)
256	18.112	0.013302	(18.086, 18.138)	18.099	0.0050811	(18.089, 18.109)
512	18.078	0.013281	(18.052, 18.104)	18.064	0.0051171	(18.054, 18.074)
1024	18.031	0.013254	(18.005, 18.057)	18.026	0.0051564	(18.016, 18.037)

Table 9: Results for Barrier $U = 160$

n	Crude Monte Carlo (MC)			Antithetic Variate Monte Carlo (AVMC)		
	Price	Std Error	95% CI	Price	Std Error	95% CI
4	19.518	0.014180	(19.490, 19.546)	19.517	0.0033687	(19.511, 19.524)
8	19.476	0.014162	(19.448, 19.503)	19.486	0.0034113	(19.479, 19.492)
16	19.419	0.014135	(19.392, 19.447)	19.445	0.0034696	(19.438, 19.452)
32	19.416	0.014095	(19.388, 19.444)	19.395	0.0035299	(19.388, 19.402)
64	19.345	0.014062	(19.318, 19.373)	19.358	0.0035751	(19.351, 19.365)
128	19.336	0.014043	(19.308, 19.363)	19.325	0.0036227	(19.318, 19.332)
256	19.286	0.014023	(19.259, 19.314)	19.307	0.0036386	(19.300, 19.314)
512	19.293	0.014017	(19.266, 19.321)	19.280	0.0036826	(19.273, 19.287)
1024	19.276	0.014011	(19.249, 19.304)	19.282	0.0036739	(19.275, 19.289)

Table 10: Results for Barrier $U = 170$

The performance of antithetic variates (AVMC) in the Monte Carlo simulation demonstrates a significant improvement in both precision and efficiency when compared to the crude Monte Carlo (MC) method. Across all monitoring dates n , the standard errors obtained using AVMC are significantly lower than those from crude MC. For example, at $n = 64$ and a barrier level of $U = 160$, the standard error for crude MC is 0.013360, whereas for AVMC it is reduced to 0.0049378. A similar trend is observed at $U = 170$, where the standard error for crude MC is 0.014062, compared to 0.0035751 for AVMC. The reduction in standard error reflects the effectiveness of antithetic variates as a variance reduction technique.

The 95% confidence intervals further highlight the improved precision of AVMC over crude MC. At $n = 1024$ and $U = 160$, the crude MC confidence interval spans from 18.005 to 18.057, giving a width of 0.052. In contrast, AVMC yields a much narrower interval of 18.016 to 18.037,

with a width of 0.021. A similar pattern is seen for $U = 170$, where the confidence interval for crude MC at $n = 1024$ is (19.249, 19.304), while for AVMC it is (19.275, 19.289). These narrower intervals demonstrate the superior accuracy of AVMC, providing estimates that are generally accurate to at least two decimal places, and in some cases, close to three decimal places.

Next, we have computed the price of the continuously monitored UOC barrier option using the closed-form formula. The computed prices are as below:

Barrier Level U	Option Price
160	17.954
170	19.239

Table 11: Continuously Monitored Up-and-Out Barrier Call Option Prices

As the number of monitoring points n increases, both simulation methods demonstrate clear convergence towards the continuously monitored option price. The estimated prices decrease with increasing n , stabilising as they approach the theoretical benchmark derived from the closed-form solution. For a barrier level of $U = 160$, the crude Monte Carlo (MC) price declines from 18.636 at $n = 4$ to 18.031 at $n = 1024$, meanwhile the Antithetic Variate Monte Carlo (AVMC) price decreases from 18.617 to 18.026 over the same range. A similar convergence trend is observed for $U = 170$, where crude MC prices fall from 19.518 to 19.276, and AVMC prices converge from 19.517 to 19.282. This behaviour confirms that both simulation approaches accurately captured the convergence of discretely monitored barrier option prices towards their continuously monitored equivalents.

Figure 3 illustrates this convergence behaviour. The discrete MC and AVMC price estimates for both barrier levels progressively approach their respective continuously monitored prices (indicated by the horizontal dashed lines) as the number of monitoring dates increases. The figure further highlights the improved stability and precision of the AVMC method, particularly at higher monitoring frequencies, where its estimated prices consistently align more closely with the continuous benchmark.

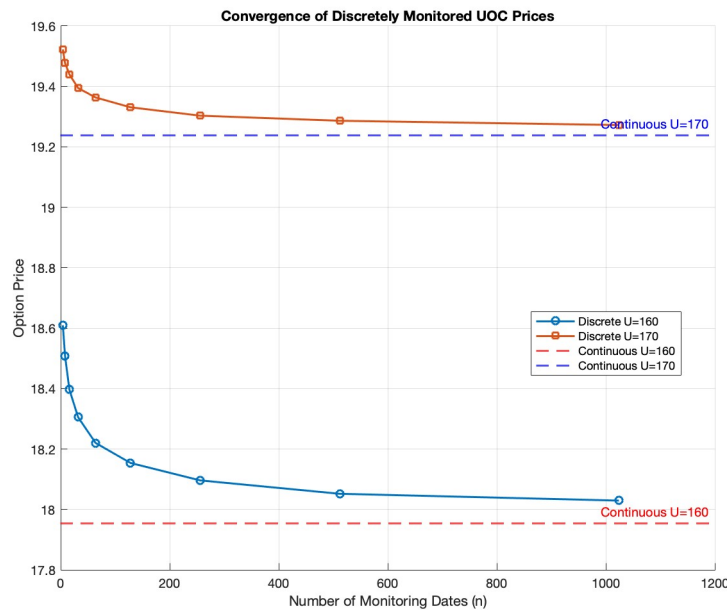


Figure 3: Convergence of Discretely Monitored UOC Prices

References

- Akos Horvath, P. M. (2016), 'Pricing asian options: A comparison of numerical and simulation approaches twenty years later', *Scientific Research* **6**. Available at: <https://doi.org/10.339>.
- Curran, M. (1994), 'Valuing asian and portfolio options by conditioning on the geometric mean price', *Management Science* **40**. Available at: <https://ssrn.com/abstract=1001473>.
- Glasserman, P. (2004), *Monte Carlo Methods in Financial Engineering*, Springer, New York.
- Xu, L., Z. H. W. F. (2023), 'Pricing of arithmetic average asian option by combining variance reduction and quasi-monte carlo method', **594**. Available at: 10.4236/jmf.2016.65056.